

Disk Drive Pivot Nonlinearity Modeling Part II: Time Domain

FEEI WANG*

Hewlett-Packard Laboratories
1501 Page Mill Road, M/S 2U
Palo Alto, CA 94304
Phone: (415) 857-7807
Email: wangf@isl.stanford.edu

TERRIL HURST

Hewlett-Packard Laboratories
1501 Page Mill Road, M/S 2U
Palo Alto, CA 94304
Phone: (415) 857-6523
Email: terril@hpl.hp.com

DANIEL ABRAMOVITCH

Hewlett-Packard Laboratories
1501 Page Mill Road, M/S 2U
Palo Alto, CA 94304
Phone: (415) 857-3806
Email: danny@hpldya.hpl.hp.com

GENE FRANKLIN

Information Systems Laboratory
Stanford University
Stanford, CA 94305
Phone: (415) 723-4837
Email: franklin@isl.stanford.edu

Abstract— This paper describes studies done at HP Labs on the actuator pivot bearing nonlinearity of a small disk drive. Part I of this paper presents a frequency-domain approach, using the swept-sine/describing function method, to obtain a model for this nonlinearity. Part II presents several additional models and discusses a time-domain approach, comparing simulated and lab measured torque versus displacement hysteresis curves. Using the measured and simulated time and frequency responses as a guide, the designer can iteratively improve the model of the system and verify the correctness of the measurements.

1. Introduction

A method using swept-sine frequency response curves for verifying measurements and models of a system containing nonlinearities was presented in [1] and [2]. Results showed a good match between the swept-sine responses of lab measurements and model simulations of the actuator pivot bearing of a small disk drive. Had this been a linear device, the modeling process would have been declared complete. However, because the device is nonlinear, a model that yields a good frequency-domain fit does not necessarily yield a good time-domain fit and vice versa. This paper presents the results and observations of time response comparisons to complement the frequency-domain modeling effort.

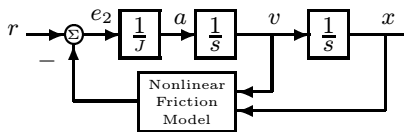


Figure 1: Simplified Block Diagram of Arm Mechanics

Several frictional models are examined here to identify a model that will best describe our system behavior. The disk drive is the same as the one considered in [1, 2]. However, the measurements shown in this paper were all taken open loop with a pivot testbed, which consists only of the actuator, including its motor, arm and pivot, with no disks present. A block diagram of the simplified system is shown in Figure 1. In addition to being nonlinear, the system is also time varying, making the modeling task more challenging and on-line adaptation desirable.

2. Lab Setup

Figure 2 illustrates the equipment configuration which was used to measure the response of the actuator pivot. A HP3567A multichannel spectrum/network analyzer was used to measure the plant response. Its source output, after a 20dB attenuation, was connected to the actuator coil leads. A laser doppler vibrometer (LDV) was used to measure the displacement of the rotary actuator's arm tip, which was covered by a strip of retroreflective tape. The signal from the LDV was then connected back to the HP3567A. For time-domain measurements, the signals were time-averaged using the excitation signal as a trigger. For frequency-domain measurements, the swept-sine measurement mode was used.

The Matlab software package was used for numerical and graphical analysis of the measurements. Time-domain plots

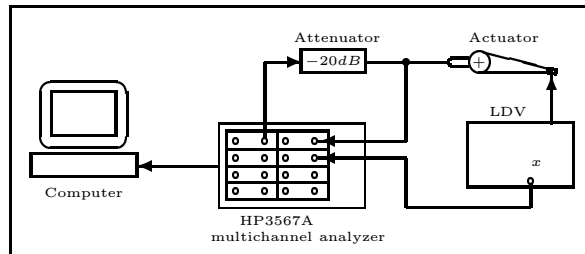


Figure 2: Equipment Setup

were generated of input voltage versus displacement, thereby displaying the nonlinear hysteresis effect depicted throughout this paper.

The preferred signal to be plotted versus displacement is actually the frictional torque. Unfortunately, it is very difficult to measure the frictional torque directly. However, it can be shown that the frictional torque is approximately proportional to the input current which is in turn approximately proportional to the input voltage¹ at low frequencies. The input voltage can therefore be used instead.

3. Modeling

A set of three swept-sine frequency response measurements and three time response measurements, taken at corresponding input amplitudes, are used as a basis of comparison in characterizing the plant. For the time response measurements, a sinusoidal input signal at 6 Hz is used. The frequency of 6 Hz is chosen because it is low enough so that the inertial term is negligible at all input amplitudes of interest, and is large enough so that simulations and measurements do not take an excessively long time.

3.1 Considerations

As stressed in Part I of this paper[2], it is important to make sure that the simulation process mimics the measurement process, taking into account characteristics of the instruments that generate the measurement results. This was more of an issue in [1] and [2] because much more complicated data processing was performed in the frequency domain measurement process. As the instrumentation does no processing of the data, apart from some averaging, in the time domain approach presented in this paper, this is of less significance.

There are several tradeoffs in selecting a suitable model. The most obvious one is how well the model predicts actual plant behavior. As mentioned earlier, because of the time-varying nature of the system, on-line identification and adaptation is desirable. Thus, the ease of identification also constitutes a major concern. To that end, the number of parameters and whether the system equations are linear in those parameters are important factors. In addition, since no system is noise-free, one needs also consider how sensitive the parameter estimations are to noise. Last but not least, another important issue is how sensitive closed-loop plant behavior is to changes in parameter values. If the plant is relatively insensitive to a particular parameter, then one can potentially treat it as a constant to simplify the task of identification.

¹As mentioned in Part I[2], for the disk drive of concern and the frequency range of interest, effects of the coil inductance and back emf are negligible, so the frequency response curve from coil voltage to armature current is relatively flat.

*Feei Wang is a Ph.D. candidate at the Information Systems Lab and is doing joint research at Hewlett-Packard Labs under HPL's intern program.

3.2 Models and Results

Several classical friction models, including preload, Dahl and hysteretic-damping models, were considered. Investigations showed that none of them can describe the plant behavior well. Thus, additional models were developed. Due to space limitations, only four of them are presented in this paper: preload plus two-slope spring, Dahl plus viscosity, hysteretic two-slope and hysteretic-damping plus preload. Notice that most of them are enhanced versions of the classical models.

The arm-mechanics block diagram used to generate simulation results is similar to the one in [1]. Simulation results for each model are plotted (in dashed lines) against the set of lab measurements aforementioned (in solid lines). When possible, the parameter values were first obtained using non-negative least-squares fit, then fine-tuned iteratively.

3.2.1 Preload plus Two-Slope Spring Model:

This model consists of a preload nonlinearity in the velocity feedback loop and a two-slope spring in the position feedback loop. A block diagram is shown in Figure 3. The SIMULINK

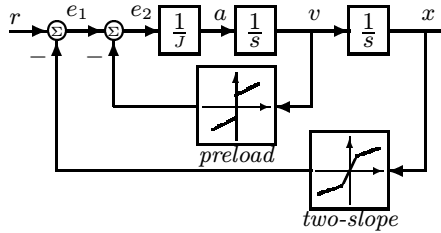


Figure 3: Preload plus Two-Slope Spring Model

simulation block diagram is included in Part I of this paper[2]. As explained there, this model is motivated by observations from the frequency response curves. The variation of low-frequency gain with amplitude prompted the two-slope position dependence, and the DC phase prompted the Coulomb component.

The equation for the frictional torque is

$$F = K_c \operatorname{sgn}(v) + K_v v + \begin{cases} K_a x, & |x| < S_a \\ K_b x + (K_a - K_b)S_a, & |x| > S_a \end{cases} \quad (1)$$

where K_c is the Coulomb level, K_v is the viscosity, K_a and K_b are the spring constants for small and large displacements respectively, and S_a is the break point in the spring stiffness. As evident in the system equation, there are five parameters in this model, and the system equation is linear in all parameters except S_a .

A sample result is shown in Figure 4, showing that a good time-domain match to measured data across multiple amplitudes can be achieved with the same set of parameters. Obtaining these parameter values from the time domain measurements was easy due to the fact that the system equation is linear in almost all parameters in this model.

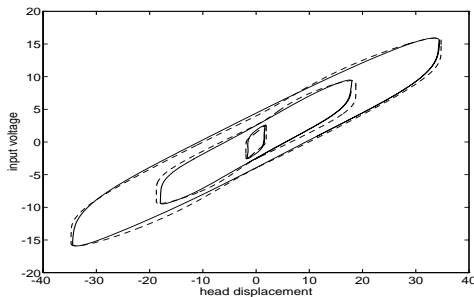


Figure 4: Measured *vs.* Simulated time response using preload plus 2-slope spring model. Dashed: simulation. Solid: measurement.

Swept-sine simulations were run using the same set of parameters that yielded the excellent fit in hysteresis curves. The

result is shown in Figure 5. The frequency-domain match is poor, with the simulated response being overdamped.

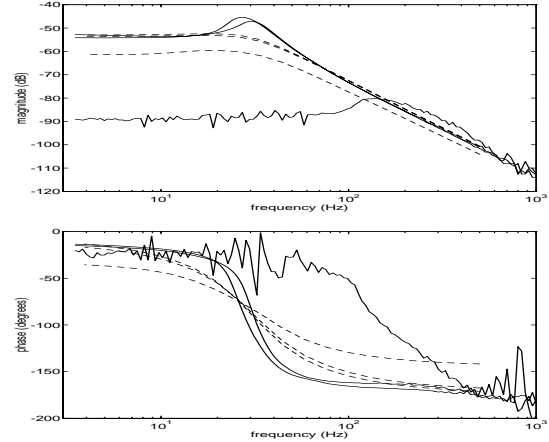


Figure 5: Measured *vs.* Simulated swept-sine frequency response using preload plus 2-slope spring model. Used parameters that gave good time-domain fit. Dashed: simulation. Solid: measurement.

Conversely, a set of parameters was obtained that generated a good swept-sine frequency response fit to the measured data, as shown in Figure 6. The same parameter values gave a poor time-domain fit however, as shown in Figure 7.

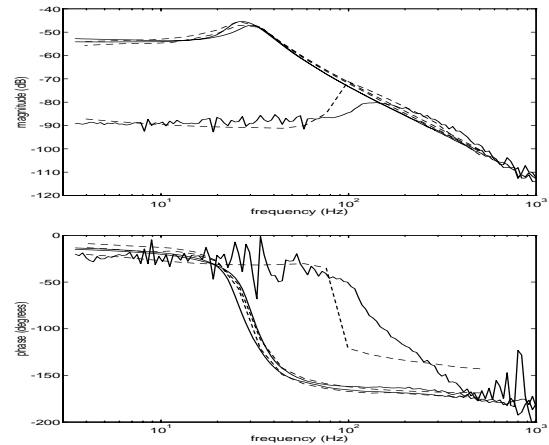


Figure 6: Measured *vs.* Simulated swept-sine frequency response using preload plus 2-slope spring model. Dashed: simulation. Solid: measurement.

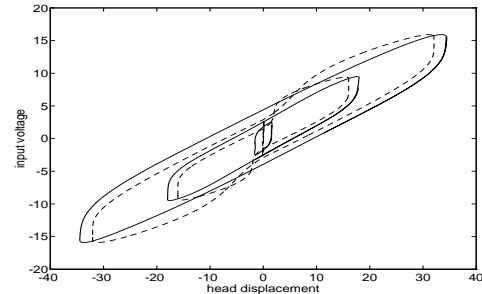


Figure 7: Measured *vs.* Simulated time response using preload plus 2-slope spring model. Used parameters that gave good frequency-domain fit. Dashed: simulation. Solid: measurement.

3.2.2 Dahl plus Viscosity Model: The Dahl model, shown in Figure 8, was empirically derived by Dahl[4,

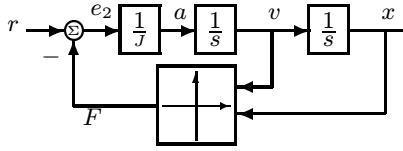


Figure 8: Classical Dahl Model

5, 6] to describe low-frequency hysteresis curves observed in ball bearings. Equation 2 is the ODE governing its behavior.

$$\frac{dF}{dx} = \sigma \left| 1 - \frac{F}{F_c} \operatorname{sgn} \dot{x} \right|^i \quad (2)$$

where

$$\begin{aligned} \sigma &= \text{rest slope,} \\ F_c &= \text{rolling torque, and} \\ i &= \text{exponential factor} \end{aligned}$$

The Dahl model has gained much recognition and usage in the mechanical engineering and aero-astro literature. However, as mentioned above, it does not describe our plant well, and an enhanced version with the addition of a viscosity term is considered.

There are now four parameters, the rest slope, the rolling torque, the exponential factor and viscosity. The equation of motion is clearly not linear in the parameters; thus, on-line identification for this model will require more effort than for the preload plus two-slope spring model.

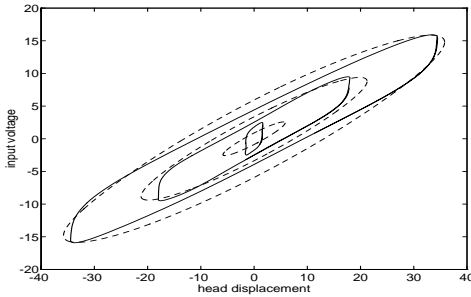


Figure 9: Measured *vs.* Simulated time response using the Dahl model plus viscosity. Dashed: simulation. Solid: measurement.

As shown in Figure 9, the Dahl plus viscosity model does not match the measured behavior well near velocity reversals. The reason that the Dahl model does not describe the observed behavior may be due to the small dimensions of the disk drive. It turns out that in our system the rolling region is actually never reached in amplitudes representative of track following. The Dahl model, while covering both the pre-rolling and the rolling regions, misses the fine details in the region very close to the origin, thus failing to describe our system. It is interesting to note that a behavior similar to the two-slope spring (as opposed to the smooth transition predicted by the Dahl model) was observed in [7] as well.

Swept-sine frequency response simulations using the Dahl model with viscosity showed no variation at all with input amplitude, so the results are not shown here.

3.2.3 Hysteretic Two-Slope Model: This model is motivated by combining the observed two-slope spring behavior and the hysteretic type behavior of the Dahl model. As Figures 6, 7 show, a good swept-sine frequency response match can be obtained using the preload plus two-slope spring model, but the hysteresis curves appear to have a “phase lag,” which causes a necking down of the hysteresis loops near zero displacement. As in the Dahl model, the steep slope should occur in the low velocity region instead of near zero displacement. The hysteretic two-slope model is an attempt to remedy this.

The block diagram of this model is shown in Figure 10. There are four parameters: the viscosity K_v , the spring stiffness near velocity reversals K_a , the spring stiffness away from

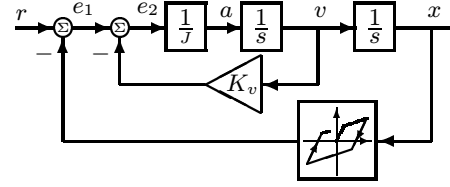


Figure 10: Hysteretic Two-Slope Model

velocity reversals K_b and the break point in the spring stiffness S_a . Although the hysteretic two-slope model has one fewer parameter than the preload plus two-slope spring model, it is no longer memoryless. On-line identification with this model will therefore be more difficult.

A sample result is shown in Figure 11. Figure 12 shows the result of swept-sine simulations using the same set of parameter values. As expected the problem of necking down of the hysteresis loops near zero displacement has disappears. However, the authors were still unable to arrive at one set of parameter values to provide a good match across multiple amplitudes in both domains simultaneously.

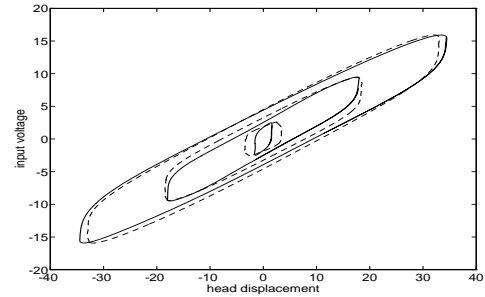


Figure 11: Measured *vs.* Simulated time response using the hysteretic two-slope model. Dashed: simulation. Solid: measurement.

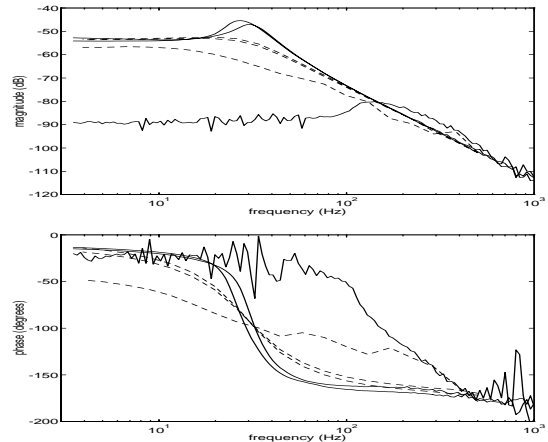


Figure 12: Measured *vs.* Simulated frequency response using the hysteretic two-slope model. Used same parameters that gave good time-domain fit. Dashed: simulation. Solid: measurement.

3.2.4 Hysteretic Damping plus Preload Model: The classical hysteretic damping model, shown in Figure 13, has been widely used in the mechanical engineering literature[8]. It is considered because it also provides a means of obtaining low-frequency hysteresis curves, as shown in Figure 14, and DC phase. The frequency response function from input $r(t)$ to output $x(t)$ is

$$\frac{X}{R}(s) = \frac{1}{Js^2 + K(1 + j\eta)}. \quad (3)$$

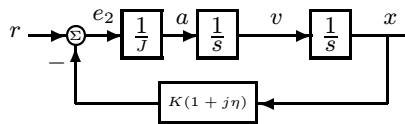


Figure 13: Classical Hysteretic Damping Model

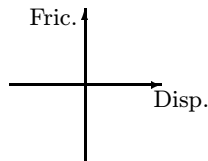


Figure 14: Typical Hysteresis Curves from Hysteretic Damping Model

Again, because the classical hysteretic damping model does not yield responses that match our measurements well, a preload term is added in the hope that it will perform better². There are four parameters in the enhanced model: the Coulomb level K_c , the viscosity K_v , the linear spring term K and the loss factor η . The system equation is linear in all the parameters.

A sample result is shown in Figure 15. The swept-sine simulation result using the same parameter values is shown in Figure 16. The high-amplitude responses appear to match quite well, but the small-amplitude match is poor.

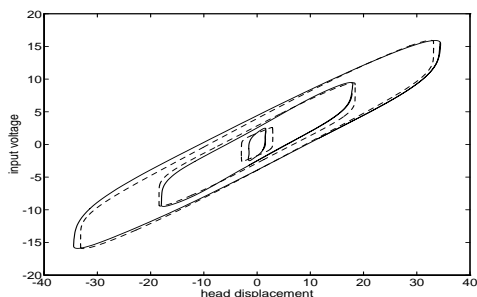


Figure 15: Measured *vs.* Simulated time response using the hysteretic-damping model with additional preload. Dashed: simulation. Solid: measurement.

4. Summary and Conclusions

This paper, together with [2], presents a method to verify system models and measurements for a strongly nonlinear system. Part I presented the frequency-domain method and Part II the time-domain. Both are integral components in nonlinear system modeling. However, there are drawbacks to both methods presented, namely, that vital information is being discarded. Pure sinusoids are used in both methods, so the type of signals we observe is limited. Nonetheless they are still useful model verification tools that help provide insight into model and plant behavior.

It is clear from [2] that a position feedback term is necessary in order to obtain the spring line observed in lab measurements. Meanwhile, the results in Part II of this paper show that the models that are position-dependent only, *i.e.*, the Dahl model and the hysteretic damping model, do not model the system well unless a velocity dependence is added. Thus, as already stated in [2], the frictional behavior is not determined solely by velocity feedback or position feedback, but by a combination of the two acting at all times.

While we have obtained models (ones containing both velocity and position dependences) that better describe the disk

²In this case, because viscosity is equivalent to an imaginary spring term when the frequency is fixed, merely adding a viscosity term will not improve the time response of the model; thus, a Coulomb component was included as well.

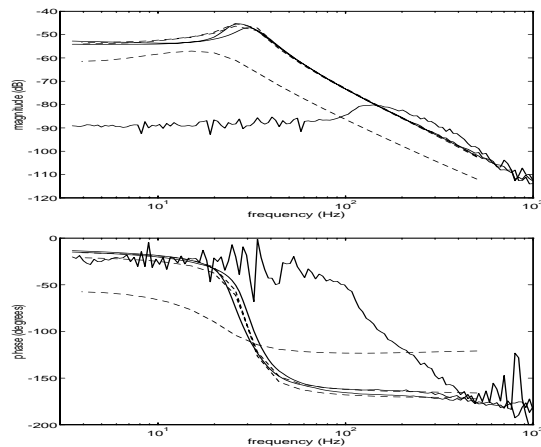


Figure 16: Measured *vs.* Simulated frequency response using the hysteretic-damping model with preload. Used parameters that gave good time-domain fit. Dashed: simulation. Solid: measurement.

drive actuator than do classical models, they still do not meet the requirement of matching measured system response in both domains simultaneously. Perhaps the assumption that velocity feedback and position feedback can be decoupled is invalid and cross terms need to be included.

5. Acknowledgements

The results discussed in this paper are the result of a team effort at HP Labs. Credit is due to Dick Henze, who helped take laboratory measurements and contributed many ideas and insights to the measurement and modeling process.

References

- [1] F. Wang, D. Abramovitch, and G. Franklin, "A method for verifying measurements and models of linear and nonlinear systems," in *Proceedings of the 1993 American Control Conference*, (San Francisco, CA), pp. 93–97, AACC, IEEE, June 1993.
- [2] D. Abramovitch, F. Wang, and G. Franklin, "Disk drive pivot nonlinearity modeling part I: Frequency Domain," in *Proceedings of the 1994 American Control Conference*, (Baltimore, MD), AACC, IEEE, June 1994.
- [3] A. Gelb and W. E. Vander Velde, *Multiple-Input Describing Functions and Nonlinear System Design*. New York: McGraw-Hill Book Company, 1979.
- [4] P. R. Dahl, "Measurement of solid friction parameters of ball bearings," in *Proceedings of the 6th Annual Symposium on Incremental Motion, Control Systems and Devices*, pp. 49–60, University of Illinois, AIAA, 1977.
- [5] P. R. Dahl, "Solid friction damping of mechanical vibrations," *AIAA Journal*, vol. 14, pp. 1675–1682, December 1976.
- [6] P. R. Dahl, "A solid friction model," Technical Report TOR-158(3107-18), The Aerospace Corporation, El Segundo, CA, May 1968.
- [7] S. Futami, A. Furutani, and S. Yoshida, "Nanometer positioning and its micro-dynamics," *Nanotechnology*, vol. 1, pp. 31–37, July 1990.
- [8] A. Nashif, D. Jones, and J. Hendersen, *Vibration Damping*. New York, NY: John Wiley & Sons, 1985.